

THE UNIVERSITY OF WARWICK

Original citation:

Bhatnagar, Akash, Kim, Young Heon, Hesse, Dietrich and Alexe, Marin. (2014) Sub-band level-assisted photoconduction in epitaxial BiFeO₃ films. Applied Physics Letters, Volume 105 (Number 12). Article number 122905

Permanent WRAP url:

<http://wrap.warwick.ac.uk/12202>

Copyright and reuse:

The Warwick Research Archive Portal (WRAP) makes this work of researchers of the University of Warwick available open access under the following conditions. Copyright © and all moral rights to the version of the paper presented here belong to the individual author(s) and/or other copyright owners. To the extent reasonable and practicable the material made available in WRAP has been checked for eligibility before being made available.

Copies of full items can be used for personal research or study, educational, or not-for-profit purposes without prior permission or charge. Provided that the authors, title and full bibliographic details are credited, a hyperlink and/or URL is given for the original metadata page and the content is not changed in any way.


Publisher statement:

<http://dx.doi.org/10.1063/1.4896508>

A note on versions:

The version presented here may differ from the published version or, version of record, if you wish to cite this item you are advised to consult the publisher's version. Please see the 'permanent WRAP url' above for details on accessing the published version and note that access may require a subscription.

For more information, please contact the WRAP Team at: publications@warwick.ac.uk

warwick**publications**wrap

highlight your research

<http://wrap.warwick.ac.uk/>

Sub-band level-assisted photoconduction in epitaxial BiFeO₃ films

Akash Bhatnagar,^{1, a)} Young Heon Kim,² Dietrich Hesse,¹ and Marin Alexe^{1, 3}

¹⁾Max Planck Institute of Microstructure Physics, 06120 Halle (Saale), Germany

²⁾Korea Research Institute of Standards and Science, Daejeon 305-304, Rep. of Korea

³⁾Dept. of Physics, University of Warwick, Coventry CV8 2EN, United Kingdom

(Dated: 24 August 2014)

Sub-band level assisted conduction mechanisms are well known in the field of semiconducting materials. In this work, we explicitly show the validity of such a mechanism in the multiferroic material BiFeO₃ (BFO). Our study is based on two different systems of epitaxial thin films of BFO, relaxed and strained. By analyzing the spectral distribution of the photoresponse from both the systems, the role of the sub-band levels in the photoconductive phenomena becomes evident. Additionally, the influence of epitaxial strain on the trapping activity of these levels is also observed. A model is proposed by taking into account the reversal of the role of a sub-band gap level, i.e. from a trapping to a ground state.

The recent discovery of an abnormal photovoltaic effect (APV) in epitaxial BiFeO₃ (BFO) films has largely revived the field of photoferroelectric materials.¹ Initial studies attributed the APV effect in BFO films to an efficient separation of photogenerated carriers at the domain walls.² Subsequent microscopic and macroscopic studies revealed the actual mechanism behind the APV effect to be the bulk photovoltaic effect (BPV).^{3,4} BPV effect in the past has been studied in other non-centrosymmetric materials, which are also ferroelectric, like BaTiO₃,⁵ LiNbO₃⁶ and KNbO₃.⁷ Theoretical studies, based on an analysis of the Boltzmann transport equation⁸ and on first principle calculations,⁹ predict primarily two conditions for the manifestation of the BPV effect in non-centrosymmetric materials. First, an asymmetric generation of charge carriers in *k*-space is required, that is realized due to the asymmetric structure of ferroelectric materials.^{7,8} Second, the recombination processes must proceed in a different way than the carrier excitation process,⁸ in other words the recombination process must be different from a simple band-band recombination. The presence of sub-band levels can apparently assist in fulfilling the second condition. Hence, it is rather essential to study the presence and activity of these levels within the band gap of BFO. Studies have shown the existence of sub-band levels in BFO,^{10–12} but their activity has been largely under discussion. Nevertheless, the effect of these levels on the generation and recombination times of the photogenerated carriers has been shown.³

In this work we conclusively show the existence of these sub-band levels in epitaxial BiFeO₃ films and demonstrate their impact on the photoconduction mechanism. We make use of two symmetries of BFO to investigate the role of these levels. We then propose a band model to explain the activity of these levels.

Approximately 100 nm thick single crystalline BFO films were deposited on two different substrates, namely TbScO₃ (TSO) and LaAlO₃ (LAO). The orientation for either of the substrates was chosen to be (001) in the

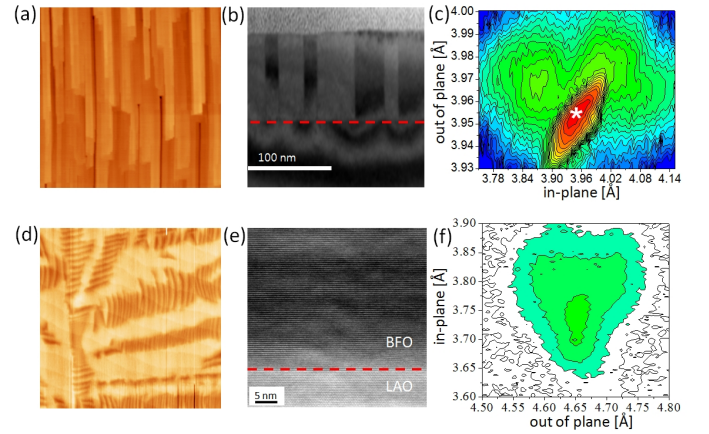


FIG. 1. Structural characterization for a BFO film deposited on TSO showing (a) AFM topography image of $4 \times 4 \mu\text{m}$ area, (b) cross-sectional TEM image displaying 109° domains, (c) RSM measured around $(103)_{pc}$ with the peak from the substrate indicated by a white star. Structural characterization for a BFO film deposited on LAO showing (d) AFM of $3 \times 3 \mu\text{m}$ area, (e) cross-sectional TEM image of a region free from the stripes shown in (d), (f) RSM measured around $(103)_{pc}$ with the peak from the substrate not visible.

pseudo cubic notation (index "pc"). The BFO films were fabricated by pulsed laser deposition with a laser energy density of approximately 0.35 J/cm^2 and a substrate temperature of 650°C . The films were gradually cooled down under an oxygen partial pressure of 200 mbar. Platinum electrodes, $250 \mu\text{m}$ in length with a gap of $15 \mu\text{m}$, were patterned on top of the BFO films by following conventional lithography, sputtering and lift-off processes. Figure 1 shows AFM images of the surface morphology and cross-sectional TEM micrographs obtained from films deposited on TSO and LAO substrates, respectively. Typical 109° domain boundaries are visible in the cross-section TEM image (Fig. 1(b)) obtained from the BFO film grown on TSO.¹³ The morphology of the BFO film grown on LAO (Fig. 1(d)) shows stripe-like features that are embedded in the matrix of the monoclinic phase. The stripes represent a mixture between the monoclinic

^{a)}Electronic mail: bhatnaga@mpi-halle.mpg.de

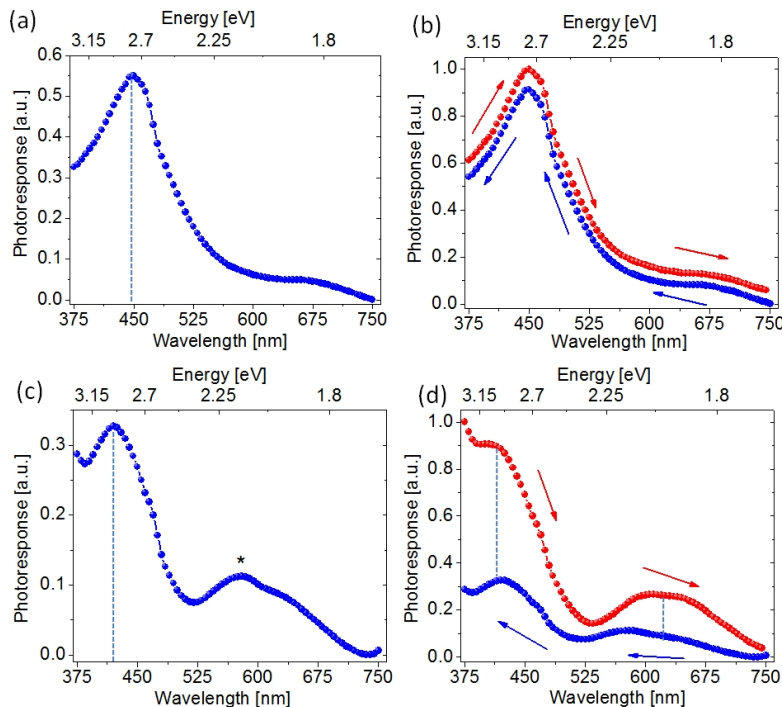


FIG. 2. Spectral response obtained from the rhombohedral film (a) for the first cycle when the wavelength is changed from 750 to 375 nm. (b) for both cycles. Spectral response obtained from the monoclinic film (c) for the first cycle when the wavelength is changed from 750 to 375 nm. (d) for both cycles. The photoresponse was measured under an applied bias voltage of 20 V.

and the rhombohedral-like phases of BFO.¹⁴ The reciprocal space maps (RSM) measured around the $(103)_{pc}$ peak of the BFO films grown on TSO (Fig. 1(c)) and LAO (Fig. 1(f)) reveal an out-of-plane lattice constant of 3.96 Å and 4.61 Å, respectively. It has been previously shown that the BFO crystallizes in a rhombohedral structure on TSO,¹⁵ whereas it mainly adopts a monoclinic structure (M_c) when grown on LAO.¹⁶ The monoclinic structure of the BFO film grown on LAO substrate can be identified by the three-fold splitting of the peak from BFO (Figure 1(f)).^{16,17}

Further on, the spectral response was measured in the photoconductive mode by using a Xenon white lamp in tandem with a monochromator. The electrode gap was uniformly illuminated with monochromatic light of variable wavelength. The photocurrent was recorded under a constant bias voltage, via a high impedance electrometer (Keithley 6517). The measurements were performed at room temperature and comprised of two cycles of wavelength scanning. In the first cycle, the wavelength was scanned from 750 to 375 nm and in the second cycle from 375 to 750 nm. The wavelength was changed by 5 nm after every 5 seconds, during both the cycles. The bias voltage was maintained during either of the cycles. The photocurrent recorded at each value of the wavelength was normalized with the power available at that wavelength to obtain an effective spectral distribution of the photo response.¹⁸

Figures 2(a, b) and 2(c, d) show the photoresponse

obtained from the rhombohedral and monoclinic BFO film, respectively. Figure 2(a) shows the response from the rhombohedral film acquired during the first cycle of wavelength scanning. A number of observations can be made from the response. Firstly the peak in the response appearing at a wavelength of 450 nm can be attributed to the photoconduction occurring via band-band transition of photo generated carriers. This yields a band gap value of approx 2.75 eV and is in accordance with previously reported values.¹⁹ Secondly, the onset of photoconduction happens at an energy that is clearly smaller than the actual band gap. Although it is not possible to well define the value of the onset, it can be approximated to be around 2.4 eV. Figure 2(b) shows the acquired photoresponse when the wavelength is scanned from 375 to 750 nm. The response in this cycle is identical to that of the first cycle ; however a slight increment is observed at the position of the band gap value (450 nm).

The onset of photoconduction at 2.4 eV is a clear indication of the presence of a level, or a band of levels, just below the conduction band. The effect of these levels on the recombination and generation of photo-generated processes has been initially revealed by microscopic studies.³ Nevertheless, these levels are in thermal equilibrium with the conduction band, which is evident from Figure 2b since the second cycle response is identical to the first cycle response. Thus the trapping effects are not significant or are of very short time.

The situation is somehow different in the case of

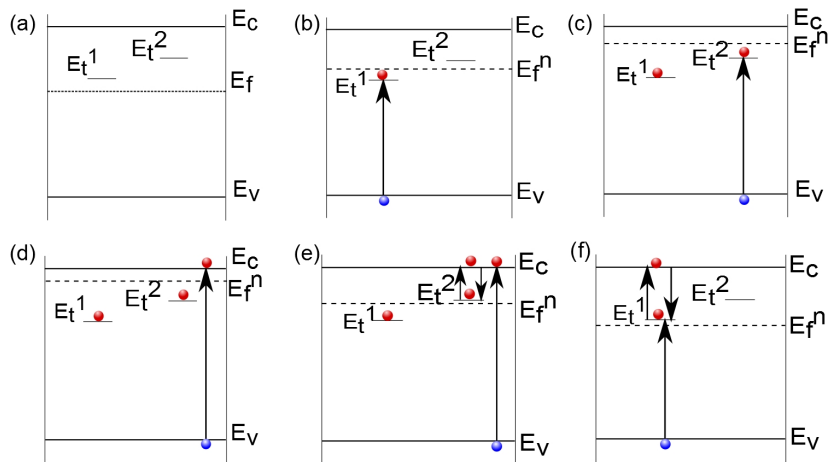


FIG. 3. Schematic of the band diagrams (not to the scale) when (a) the film is in equilibrium, (b) the wavelength is varied from 715 to 500 nm and electrons are excited to E_t^1 level, (c) the wavelength begins to decrease below 500 nm and the electrons are excited to E_t^2 level, (d) the wavelength reaches the band gap energy and there is band-band excitation, (e) the wavelength is scanned from 375 to 500 nm in the second cycle and the level E_t^2 is in thermal equilibrium with the E_c , (f) the wavelength scans from 500 to 715 nm in the second cycle and the level E_t^1 is in thermal equilibrium with the E_c .

strained BFO. In Figure 2(c), the response acquired during the first cycle of wavelength scanning (from 750 to 350 nm) from the monoclinic BFO film is presented. Similar to the case of rhombohedral BFO (Figure 2(a)), the peak in the response can be attributed to photoconduction via band-band transitions. However in the case of strained BFO, the band gap value is approximately 2.95 eV, which is about 0.2 eV higher than the band gap for the rhombohedral BFO film. Interestingly, a rather broad peak appears around 575 nm as is indicated by a star in Figure 2(c). The peak stretches from 650 to 525 nm which indicates the presence of either two levels or of a continuous band of levels. After this broad peak, the response further decreases with the wavelength up to 505 nm (2.4 eV) where the response begins to increase again. Thereafter, the response continues to increase up to 420 nm when the photoconduction is occurring via band-band transition.

Figure 2(d) shows the response measured during the second cycle of wavelength scanning from high to low energy (375 to 750 nm). The response in the second cycle resembles the first cycle response, but there is a considerable enhancement. The response is approximately 2.7 times higher around the wavelength that corresponds to the supposed band gap value and 3 times higher in the region of the deep sub-band peak.

A number of comparisons can be made between the responses from the rhombohedral and monoclinic BFO films. First, the band gap in the rhombohedral film is approximately 0.2 eV lower than in the monoclinic film. Second, in either of the films the onset of photoconduction is approximately from 2.4 eV and increases continuously until the photoconduction occurs via band-band transition. This shows the existence of certain levels, or a band of levels, just below the conduction band in either of the films. The absence of a well-defined or a distinct peak suggests that these levels are apparently in close

proximity with the conduction or valence band. But the much higher response observed during the second cycle in the monoclinic film is a clear indication of an influence of sub-band levels on the photoconduction mechanism in strained BFO. The increase of the photoresponse can be understood, assuming the presence of an active trap level and making use of the concept of quasi Fermi levels.²⁰

The enhanced response obtained in the second cycle of the monoclinic film can be explained by the band diagram schematically shown in Figure 3. Under steady state conditions, the Fermi level (E_f) of the system can be considered to be positioned close to the conduction band (E_c), assuming electrons as the majority carriers and considering strained BFO as an n-type semiconductor (Figure 3(a)). But when the system is subjected to an illumination, the E_f of the system splits into quasi Fermi levels for holes (E_f^h) and electrons (E_f^n). In the schematic shown in Figure 3(b), only the level (E_f^n) is shown. The transition that might be responsible for the peak obtained around 600 nm is shown in Figure 3(b). A discrete trapping level at the energy E_t^1 , which under steady state conditions is placed above E_f^n , gets charged with electrons when under illumination of a wavelength of approximately 600 nm. The resulting free holes generated in the valence band (E_v) are at the origin of the broad peak in the photoresponse. As the photon energy is increased, the carriers from E_v are excited to another sub-band level at the energy E_t^2 (Figure 3(c)). Accordingly, the level E_f^n moves to above E_t^2 . The proximity of this level to the bottom of the conduction band does not result in a distinct peak in the response. Nevertheless, the free holes generated in the valence band contribute to the measured photoresponse. Gradually the energy of the illuminating light is further increased, and finally equals the band gap (Figure 3(d)). This results in the generation of free electrons in the conduction band and

free holes in the valence band that yields in a sudden rise in the photoresponse. One may also speculate on the trapping of carriers by the two discrete levels during this process.

It is noteworthy to mention here the character of such sub-band levels. Rose in his seminal work on photoconductors and insulators²¹ categorized these levels as either ground states or trap levels, based upon their position with respect to the quasi Fermi levels. A level is denoted as ground state if it lies below the quasi Fermi level and as a trapping level if the quasi Fermi level is positioned below it. The carriers trapped in the ground state will have a higher probability to be recombined before they can be thermally released into one of the allowed bands. Nevertheless, the redistribution of the carriers amongst these ground states results in the establishing of the inherent equilibrium state of the system. On the other hand, the carriers in the trap level are quickly re-excited into the allowed bands. Additionally, the activity of the trap levels results in a higher lifetime of the carriers because the recombination occurs via these levels, and hence is delayed. Interestingly, the character of such sub-band levels can be changed or tuned either by light or temperature. In this way, a ground state can become a trap level, or vice versa, when the quasi Fermi level is moved either by light or temperature.²² Hence, in the first cycle, by sequential increase of the illumination energy, the levels at E_t^1 and E_t^2 were transformed into ground states and were charged with carriers.

We can now proceed with our explanation of higher response obtained for the second cycle. In the second cycle the energy is sequentially decreased, and the recombination processes are activated. As a result, the E_f^n level begins to move back towards the middle of the band gap, and the electrons - which were previously captured at level E_t^2 - get into equilibrium with the band E_c (Figure 3(e)). Alternatively, the nature of level E_t^2 changes from ground to trap state. This releases additional carriers, that are now available for the photoconduction, or even can be thermally activated and are then available for the normal conduction process. Also, the lifetime of the carriers is enhanced, because recombination now proceeds via the level. Due to the combined effect, there is an overall increase in photoconductivity and hence in the photoresponse. As the energy decreases further, the E_f^n level continues to fall back to retain its steady state position, and the level E_t^1 is encountered (Figure 3(f)). The carriers previously trapped in this level are also released, which yields a higher current than the one observed in the first cycle. Hence the photoconduction in strained BFO is affected by sub-band levels.

It is rather intriguing that the sub-band levels have such a large effect on the photoconduction mechanism in the strained (monoclinic) BFO film and not in the relaxed (rhombohedral) film. One of the reasons could be the variation of the capture cross-section of the trap levels. The capture cross-section of a trap level is defined by the ability of a level to capture and remit the carriers. Also,

the capture cross-section is determined by the potential surrounding the level.²³ One might speculate here that due to a different atomic arrangement of atoms in the monoclinic films, the capture cross section of the sub-band levels is largely affected and consequently there is an evident change in the photoconduction mechanism.

In conclusion, in this work we show a sub-band level assisted photoconduction mechanism in BiFeO₃. Via photoconductive measurements we demonstrate that the activity of sub-band levels in rhombohedral and monoclinic films is very different due to the strain state. A band model has been proposed to explain the enhanced responses in the strained (i.e. monoclinic) films. The charging of the sub-band level under illumination and their subsequent emptying by tuning the position of the quasi Fermi level is the possible origin of the enhanced responses.

- ¹J. Kreisel, M. Alexe, and P. A. Thomas, *Nature Materials* **11**, 260 (2012).
- ²S. Y. Yang, J. Seidel, S. J. Byrnes, P. Shafer, C.-H. Yang, M. D. Rossell, P. Yu, Y.-H. Chu, J. F. Scott, J. W. Ager, L. W. Martin, and R. Ramesh, *Nature Nanotechnology* **5**, 143 (2010).
- ³M. Alexe, *Nano Letters* **12**, 2193 (2012).
- ⁴A. Bhatnagar, A. R. Chaudhuri, Y. H. Kim, D. Hesse, and M. Alexe, *Nature Communications* **4** (2013), 10.1038/ncomms3835.
- ⁵W. Koch, R. Munser, W. Ruppel, and P. Würfel, *Solid State Communications* **17**, 847 (1975).
- ⁶A. M. Glass, D. von der Linde, and T. J. Negran, *Applied Physics Letters* **25**, 233 (1974).
- ⁷P. Günter, *Ferroelectrics* **22**, 671 (1978).
- ⁸W. Ruppel, R. Von Baltz, and P. Würfel, *Ferroelectrics* **43**, 109 (1982).
- ⁹S. M. Young, F. Zheng, and A. M. Rappe, *Physical Review Letters* **109**, 236601 (2012).
- ¹⁰A. J. Hauser, J. Zhang, L. Mier, R. A. Ricciardo, P. M. Woodward, T. L. Gustafson, L. J. Brillson, and F. Y. Yang, *Applied Physics Letters* **92**, 222901 (2008).
- ¹¹Y. Yamada, T. Nakamura, S. Yasui, H. Funakubo, and Y. Kanemitsu, *Physical Review B* **89**, 035133 (2014).
- ¹²J. Zhang, M. Rutkowski, L. W. Martin, T. Conry, R. Ramesh, J. F. Ihlefeld, A. Melville, D. G. Schlom, and L. J. Brillson, *Journal of Vacuum Science & Technology B: Microelectronics and Nanometer Structures* **27**, 2012 (2009).
- ¹³C. T. Nelson, B. Winchester, Y. Zhang, S.-J. Kim, A. Melville, C. Adamo, C. M. Folkman, S.-H. Baek, C.-B. Eom, D. G. Schlom, L.-Q. Chen, and X. Pan, *Nano Letters* **11**, 828 (2011).
- ¹⁴Y. H. Kim, A. Bhatnagar, E. Pippel, M. Alexe, and D. Hesse, *Journal of Applied Physics* **115**, 043526 (2014).
- ¹⁵C. M. Folkman, S. H. Baek, H. W. Jang, C. B. Eom, C. T. Nelson, X. Q. Pan, Y. L. Li, L. Q. Chen, A. Kumar, V. Gopalan, and S. K. Streiffer, *Applied Physics Letters* **94**, 251911 (2009).
- ¹⁶Z. Chen, Z. Luo, C. Huang, Y. Qi, P. Yang, L. You, C. Hu, T. Wu, J. Wang, C. Gao, T. Sritharan, and L. Chen, *Advanced Functional Materials* **21**, 133 (2011).
- ¹⁷A. R. Damodaran, C.-W. Liang, Q. He, C.-Y. Peng, L. Chang, Y.-H. Chu, and L. W. Martin, *Advanced Materials* **23**, 3170 (2011).
- ¹⁸D. C. Coffey and D. S. Ginger, *Nature Materials* **5**, 735 (2006).
- ¹⁹J. F. Ihlefeld, N. J. Podraza, Z. K. Liu, R. C. Rai, X. Xu, T. Heeg, Y. B. Chen, J. Li, R. W. Collins, J. L. Musfeldt, X. Q. Pan, J. Schubert, R. Ramesh, and D. G. Schlom, *Applied Physics Letters* **92**, 142908 (2008).
- ²⁰W. Shockley and J. W.T. Read, *Physical Review* **87**, 835 (1952).
- ²¹A. Rose, *Physical Review* **97**, 322 (1955).
- ²²T. Feng, *Physical Review B* **25**, 627 (1982).

²³R. H. Bube, Photoconductivity of Solids (New York: John Wiley & Sons, INC., 1960).